Quantitative Biology 2022, 10(4): 390–402
https://doi.org/10.15302/J-QB-021-0266

RESEARCH ARTICLE

Decoding fear of negative evaluation from brain morphology: A machine-learning study on structural neuroimaging data

Chunliang Feng[1,2], Frank Krueger[3,4], Ruolei Gu[5,6,*], Wenbo Luo[7,*]

[1] Key Laboratory of Brain, Cognition and Education Sciences (South China Normal University, Ministry of Education), Guangzhou 510631, China
[2] Guangdong Provincial Key Laboratory of Mental Health and Cognitive Science, Center for Studies of Psychological Application, School of Psychology, South China Normal University, Guangzhou 510631, China
[3] School of Systems Biology, George Mason University, Fairfax, VA 22030, USA
[4] Department of Psychology, George Mason University of Mannheim, Mannheim 68159, Germany
[5] Key Laboratory of Behavioral Science, Institute of Psychology, Chinese Academy of Sciences, Beijing 100101, China
[6] Department of Psychology, University of Chinese Academy of Sciences, Beijing 100101, China
[7] Research Center of Brain and Cognitive Neuroscience, Liaoning Normal University, Dalian 116029, China
* Correspondence: luowb@lnnu.edu.cn; gurl@psych.ac.cn

Received January 13, 2021; Revised March 14, 2021; Accepted May 26, 2021

***Background*: Fear of negative evaluation (FNE), referring to negative expectation and feelings toward other people's social evaluation, is closely associated with social anxiety that plays an important role in our social life. Exploring the neural markers of FNE may be of theoretical and practical significance to psychiatry research (*e.g.*, studies on social anxiety).**

***Methods*: To search for potentially relevant biomarkers of FNE in human brain, the current study applied multivariate relevance vector regression, a machine-learning and data-driven approach, on brain morphological features (*e.g.*, cortical thickness) derived from structural imaging data; further, we used these features as indexes to predict self-reported FNE score in each participant.**

***Results*: Our results confirm the predictive power of multiple brain regions, including those engaged in negative emotional experience (*e.g.*, amygdala, insula), regulation and inhibition of emotional feeling (*e.g.*, frontal gyrus, anterior cingulate gyrus), and encoding and retrieval of emotional memory (*e.g.*, posterior cingulate cortex, parahippocampal gyrus).**

***Conclusions*: The current findings suggest that anxiety represents a complicated construct that engages multiple brain systems, from primitive subcortical mechanisms to sophisticated cortical processes.**

Keywords: fear of negative evaluation; social anxiety; structural magnetic resonance imaging; machine learning; relevance vector regression

Author summary: The current findings indicate that fear of negative evaluation, an anxiety-related trait, could be decoded from the structural features of individual brains. These findings advance our understanding on the neural signatures of anxiety and implicate potential clinical applications of brain imaging measures.

INTRODUCTION

Social anxiety refers to a persistent fear of being involved in social or performance contexts that are exposed to unfamiliar people and/or potential scrutiny by others [1]. Fear of negative evaluation (FNE) is considered to be a core feature of social anxiety and social anxiety disorder (SAD) in many clinical theories

such as the cognitive-behavioral models [2,3]. This psychological construct consists of one's feelings of apprehension about others' evaluations, one's expectation of being evaluated negatively by others, and distress over those negative evaluations [4], all of which are critical to the pathogenesis and progression of irrational social anxiety [5]. FNE and social anxiety are strongly interrelated. On one hand, people with a higher level of FNE show an interpretation bias of identifying others' emotional expressions in a negative way, which may explain their susceptibility to social anxiety [6]. On the other hand, socially anxious individuals exhibit a variety of "safety" activity, as behavioral manifestations of FNE, to avoid potential negative social judgment; for instance, they might avoid speaking or control body movement in social encounters [7]. At the clinical level, Carleton *et al.* found that FNE score is consistently higher among all patients with a (principal or additional) diagnosis of SAD compared to other diagnostic groups [5]. Though FNE and social anxiety are closely related, these two concepts are not homogeneous: according to Weeks *et al.*, FNE pertains to the sense of dread associated with being evaluated negatively in social situations, whereas social anxiety pertains to affective reactions to those situations [8]. Regarding that, although many neuroscience studies have been devoted to investigate social anxiety [9], it would still be necessary to explore the neural basis of FNE (which is largely known in the literature).

Here, we first introduce the key brain regions of general anxiety and social anxiety; we expect that some of these regions are also involved in FNE. The amygdala and the medial prefrontal cortex (mPFC), two key nodes in the "fear circuit" (refering to its significance in fear conditioning and extinction) [10–12], are widely believed to be essential for anxiety [13–15]. According to Bishop, threat-related anxiety response emerging from the amygdala is top-down regulated by the mPFC; thus, excessive anxiety is associated with amygdalar hyper-responsivity as well as frontal hyporesponsivity [14]. Both structural and functional connectivity of the amygdala-prefrontal circuitry predict individual level of anxiety [16,17]. Aside from the amygdala, Paulus and Stein pointed out that the anterior insula also influences the processes of initiating and maintaining anxious affect [18–20]. All of these brain areas play important roles in clinical and non-clinical social anxiety [21–25]. It should be noted that the neural underpinnings of social anxiety also represent some uniqueness. For instance, the ventral striatum (a key area for reward encoding in the brain, including social rewards) [26,27] shows decreased activation among SAD patients, though this region is not traditionally regarded as a key component of the anxiety circuit [25,28].

These classic findings have been widely acknowledged in the anxiety literature [29,30]. Taking a step further, recent studies have linked anxious pathology with disturbances in a distributed set of cortical and subcortical regions, including (but not limiting to) the anterior cingulate gyrus, mid-cingulate cortex, orbitofrontal cortex, thalamus, hypothalamus, hippocampus, bed nucleus of the stria terminalis, and ventral tegmental area [31–33]. The aforementioned brain areas might not be directly involved in the generation and regulation of anxiety response, but participate in other cognitive processes that help maintain anxiety symptoms, such as the encoding of uncertainty and uncontrollability [32]. Inspired by these new understandings, the current study searches for potentially relevant biomarkers of FNE in the whole brain rather than focusing on selected regions of interest (*e.g.*, amygdala, mPFC, and anterior insula) from the anxiety literature [33].

To achieve this goal, we implemented a data-driven and machine-learning-based analysis approach that takes advantage of complexity in the underlying data set, *i.e.*, multivariate relevance vector regression (RVR) on structural brain imaging data [34]. The RVR, a sparse kernel method formulated in a Bayesian framework [35], takes all neurobiological features together to determine their relationships beyond individual values [36]. Specifically, multiple morphological features of the data (*e.g.*, gray matter volume and cortical thickness; see next section for details) were derived across the whole brain to predict self-reported FNE score. The value of this approach to clinical science has been appreciated, since its multivariate nature provides valuable insights into the multifactorial etiology of clinical disorders, and enables the detection of subtle and spatially distributed effects compared to traditional univariate methods [37–40]. Using the same approach, we recently have revealed white matter structural connectivity underlying dispositional worry [41]. In this study, we expected to observe multidimensional neuroanatomical patterns associated with FNE. In light of the literature (see above), we hypothesized that the amygdala, mPFC, anterior insula, and ventral striatum were likely to be involved, but did not rule out unexpected findings since our methodology is data-driven.

RESULTS

Multivariate RVR analysis

The application of RVR to the combined morphological features allowed individualized prediction of the fear of negative evaluation scale (BFNE) scores (MAE = 6.69, $P < 0.001$; $r = 0.27$, $P < 0.001$; Fig. 1). Prediction

performance became worse when using the single-type metric (Table 1).

Contributing morphological features

Contributing features were selected, including 15 cortical thickness features, 9 gray matter volume features, 12 surface area features, 23 sulcal depth features, and 1 subcortical volume feature (Fig. 2, Table 2). The 15 cortical thickness features were derived from the following regions: left orbital gyrus, superior parietal gyrus, right middle frontal sulcus, fronto-marginal gyrus and sulcus, lateral sulcus, bilateral posterior cingulate gyri, occipital sulci and gyri, and temporal gyri. The 9 gray matter volume features were derived from the following regions: left lateral sulcus, temporal gyri, bilateral insula, and occipital gyrus and sulcus. The 12 surface area features were derived from the following regions: left orbital sulcus, lateral sulcus, posterior cingulate gyrus, subcallosal gyrus, calcarine sulcus, right insula, parahippocampal gyrus, superior parietal

Table 1 Results of RVR prediction using combined morphological features or a single morphological feature

Features	*MAE*	*P*(*MAE*)	*r*	*P*(*r*)
Combined	6.69	<0.001	0.27	<0.001
Gray matter volume	6.98	0.07	0.12	0.019
Cortical thickness	6.87	0.026	0.23	<0.001
Sulcal depth	7.84	0.997	–0.078	0.79
Surface area	6.86	0.012	0.11	0.031
Subcortical volume	5.92	0.68	–0.51	1

LOSOCV, leave-one-subject-out cross-validation; MAE, mean absolute error.

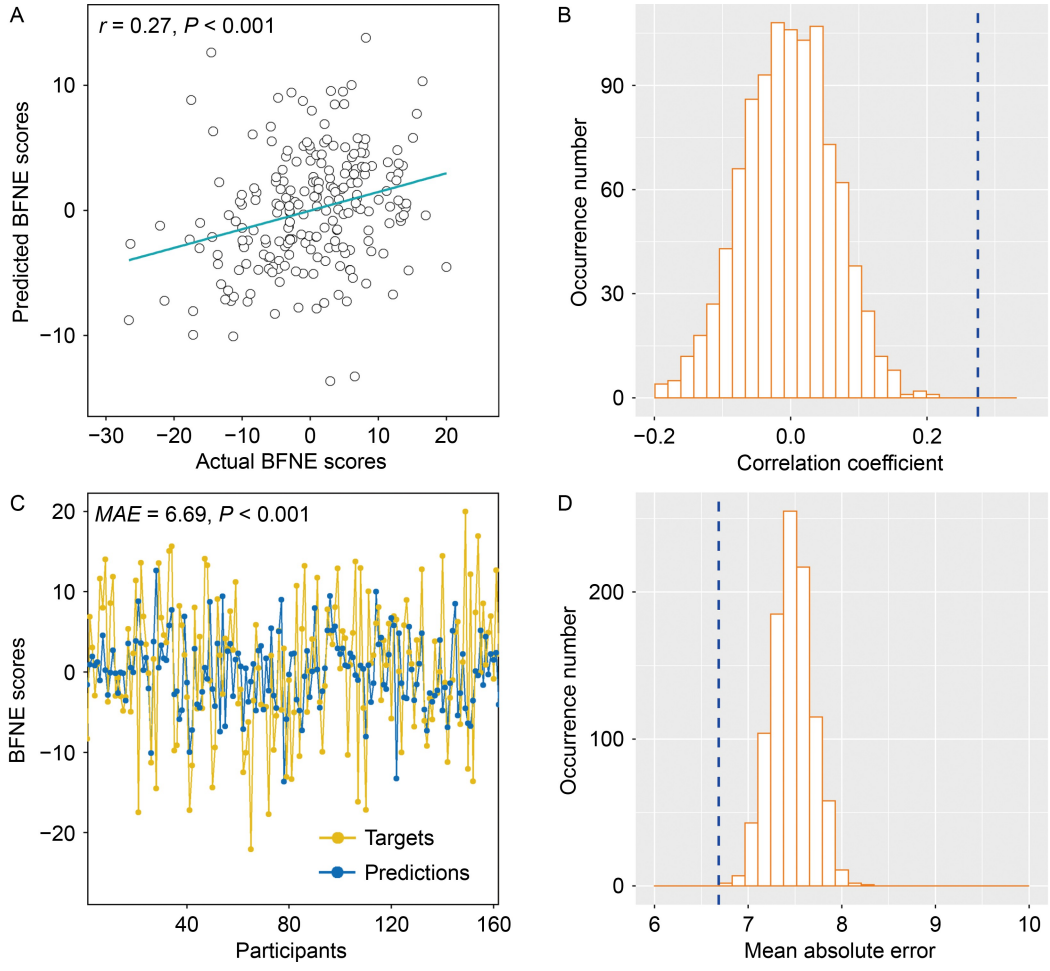

Figure 1. RVR findings of the multivariate regression analysis in BFNE score prediction using leave-one-subject-out cross-validation procedures. (A) Correlation between actual and predicted BFNE scores. (B) Permutation distribution of the correlation coefficient (*r*) with blue dashed line indicating value obtained from real scores. (C) Consistency between actual and predicted BFNE scores. (D) Permutation distribution of the mean absolute error with blue dashed line indicating value obtained from real scores. RVR, relevance vector regression; BFNE, brief version of the fear of negative evaluation scale.

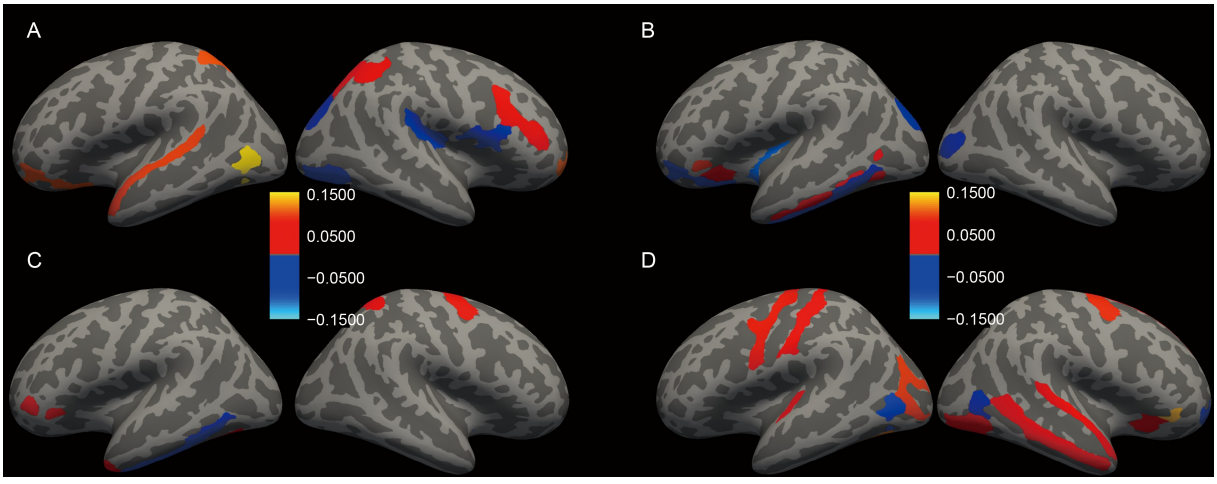

Figure 2. Morphological features contributing to the prediction of BFNE score. (A) Cortical thickness. (B) Gray matter volume. (C) Surface area. (D) Sulcal depth. BFNE, brief version of the fear of negative evaluation scale.

Table 2 Contributing morphological features with an absolute weight score higher than 10% of the maximum absolute weight value for RVR to predict dispositional fear of negative evaluation

Brain regions	Hemi.	Lobes	Metric	Weights
Orbital gyrus	L	Frontal	CT	0.080
Fronto-marginal gyrus and sulcus	R	Frontal	CT	0.109
Middle frontal sulcus	R	Frontal	CT	0.077
Posterior ramus of the lateral sulcus	R	Frontal	CT	–0.077
Opercular part of the inferior frontal gyrus	R	Frontal	CT	–0.071
Horizontal ramus of the anterior segment of the lateral sulcus	L	Frontal	GMV	0.094
Horizontal ramus of the anterior segment of the lateral sulcus	L	Frontal	SA	0.085
Medial orbital sulcus	L	Frontal	SA	0.070
Suborbital sulcus	R	Frontal	SA	0.079
Gyrus rectus	L	Frontal	SD	0.099
Precentral gyrus	L	Frontal	SD	0.082
Inferior orbital gyrus	R	Frontal	SD	0.130
Fronto-marginal gyrus and sulcus	R	Frontal	SD	–0.092
Suborbital sulcus	R	Frontal	SD	0.088
Superior frontal gyrus	R	Frontal	SD	0.080
Inferior frontal sulcus	R	Frontal	SD	0.074
Long insular gyrus and central sulcus of the insula	L	Insula	GMV	–0.109
Anterior segment of the circular sulcus of the insula	R	Insula	GMV	0.077
Anterior segment of the circular sulcus of the insula	R	Insula	SA	0.075
Inferior segment of the circular sulcus of the insula	R	Insula	SD	0.078
Posterior-dorsal part of the cingulate gyrus	L	Limbic	CT	0.073
Posterior-dorsal part of the cingulate gyrus	R	Limbic	CT	0.068
Subcallosal gyrus	L	Limbic	GMV	0.069
Parahippocampal gyrus	R	Limbic	GMV	–0.076
Posterior-dorsal part of the cingulate gyrus	L	Limbic	SA	–0.086
Subcallosal gyrus	L	Limbic	SA	0.078
Parahippocampal gyrus	R	Limbic	SA	–0.073
Subcallosal gyrus	L	Limbic	SD	0.104

(*continued*)

Brain regions	Hemi.	Lobes	Metric	Weights
Anterior part of the cingulate gyrus and sulcus	L	Limbic	SD	0.082
Pericallosal sulcus	R	Limbic	SD	0.072
Amygdala	R	Limbic	vol	–0.080
Superior parietal gyrus	L	Parietal	CT	0.077
Superior parietal gyrus	R	Parietal	SA	0.071
Subparietal sulcus	L	Parietal	SD	0.076
Lateral aspect of the superior temporal gyrus	L	Temporal	CT	0.070
Inferior temporal sulcus	R	Temporal	CT	–0.071
Inferior temporal gyrus	L	Temporal	GMV	–0.080
Superior temporal gyrus	L	Temporal	GMV	0.072
Inferior temporal gyrus	L	Temporal	SA	–0.084
Lateral occipito-temporal gyrus	L	Temporal	SA	0.070
Inferior temporal sulcus	R	Temporal	SA	0.083
Lateral occipito-temporal gyrus	L	Temporal	SD	0.117
Medial occipito-temporal gyrus	L	Temporal	SD	0.116
Lateral occipito-temporal sulcus	L	Temporal	SD	–0.095
Anterior transverse temporal gyrus	L	Temporal	SD	0.075
Lateral occipito-temporal sulcus	R	Temporal	SD	–0.072
Lateral aspect of the superior temporal gyrus	R	Temporal	SD	0.071
Middle temporal gyrus	R	Temporal	SD	0.070
Superior occipital sulcus	L	Occipital	CT	0.139
Calcarine sulcus	L	Occipital	CT	–0.096
Superior occipital sulcus	R	Occipital	CT	–0.079
Middle occipital sulcus and lunatus sulcus	R	Occipital	CT	0.076
Inferior occipital gyrus and sulcus	R	Occipital	CT	–0.074
Superior occipital gyrus	L	Occipital	GMV	–0.075
Superior occipital sulcus and transverse occipital sulcus	R	Occipital	GMV	–0.072
Calcarine sulcus	L	Occipital	SA	0.078
Middle occipital gyrus	L	Occipital	SD	0.095
Superior occipital gyrus	L	Occipital	SD	0.094
Lingual gyrus	L	Occipital	SD	–0.075
Inferior occipital gyrus and sulcus	R	Occipital	SD	0.071

Hemi., hemisphere; L, left; R, right; CT, cortical thickness; GMV, gray matter volume; SA, surface area; SD, sulcal depth; vol, volume.

gyrus, and bilateral temporal gyri and sulci. The 23 sulcal depth features were derived from the following regions: left gyrus rectus, anterior cingulate gyrus and sulcus, subcallosal gyrus, right orbital gyrus and sulcus, inferior and superior frontal gyri, insula, temporal gyri, bilateral occipital gyri and sulci, occipito-temporal gyri and sulci. The subcortical volume feature included the volume of right amygdala.

Model validation

The 10-fold cross-validation was used to re-estimate the performance of prediction. The resultant correlation coefficient and MAE values remained significant (MAE = 6.85, P = 0.004; r = 0.23, P = 0.001; Fig. 3). These results validated the main findings derived from the LOOCV approach and demonstrate the robustness of the current findings across different CV schemes.

DISCUSSION

In the current study, we utilized RVR for a better understanding of the neurobiological mechanisms of FNE. Not surprisingly, the results show that the

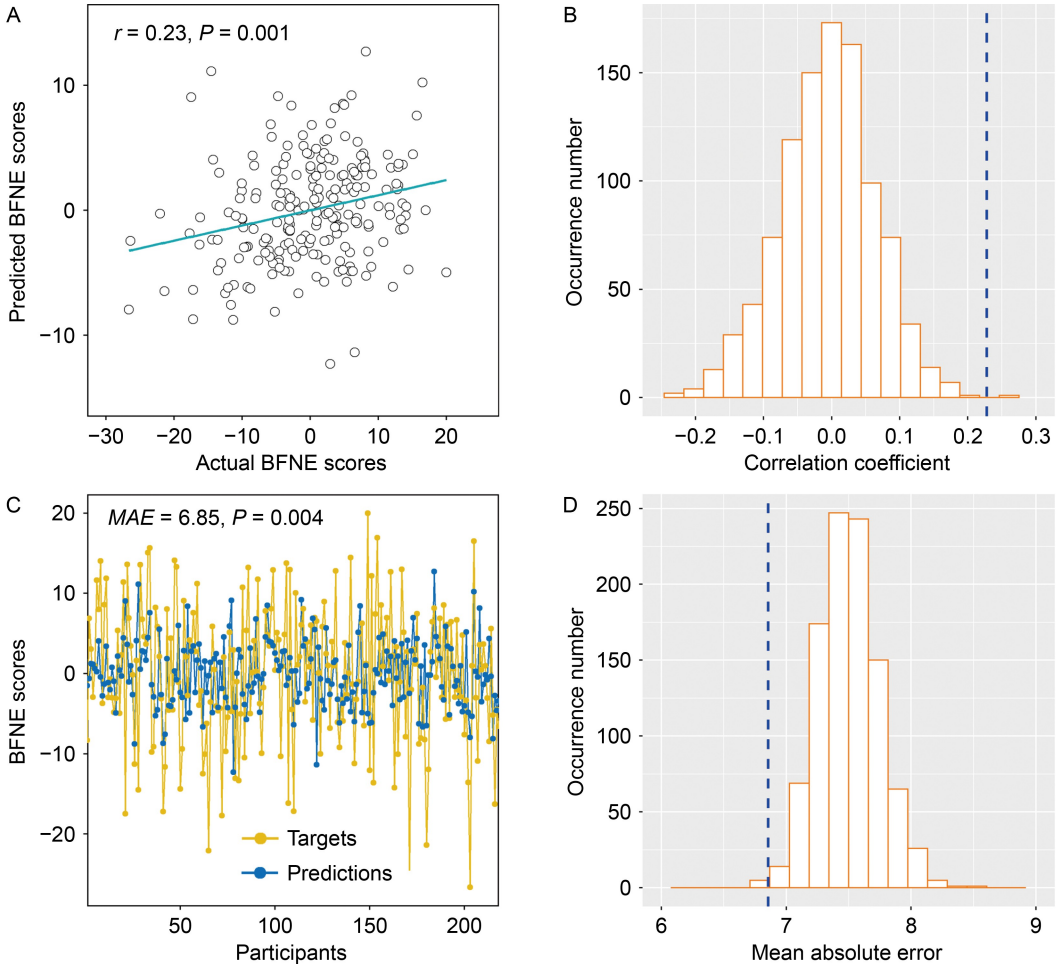

Figure 3. RVR findings of the validation analysis using 10-fold cross-validation procedures. (A) Correlation between actual and predicted BFNE scores. (B) Permutation distribution of the correlation coefficient (*r*) with blue dashed line indicating value obtained from real scores. (C) Consistency between actual and predicted BFNE scores. (D) Permutation distribution of the mean absolute error with blue dashed line indicating value obtained from real scores. RVR, relevance vector regression.

morphological features (including cortical thickness, gray matter volume, surface area, sulcal depth, and subcortical volume) of multiple regions significantly predicted FNE on the individual level (measured by BFNE score). Some of these regions (*e.g.*, the amygdala, insula, and frontal areas) have widely been considered as key parts of the "anxious brain," while others have yet to be adequately paid attention to in the literature (see the Introduction). Moreover, the robustness of the above findings has been validated.

Inspired by one of our recent studies on the imbalance between different brain networks in anxiety [42], here we first discuss the key nodes within the affective network and salience network, particularly the amygdala and insula [43–47]. It has been well established that both the amygdala and insula are related to not only general anxiety but also social anxiety, including the perception and evaluation of threatening social cues [48–51]. For example, the amygdala is activated more strongly by harsh (angry, disgusted, fearful) faces among patients with generalized social phobia, and its activation level is positively correlated with their severity of social anxiety symptoms [52,53]. In the same vein, generalized SAD patients also exhibit greater anterior insula reactivity for fear (versus happy or neutral) faces compared with healthy controls [54,55]. Here, please note that our results reveal that the insula, not just its anterior part, is associated with FNE, possibly a unique neural signature that distinguishes FNE with general anxiety or social anxiety.

In our opinion, the amygdala and insula might contribute to FNE by showing heightened sensitivity to (real or hypothetical) social evaluation such as praises and criticisms, which further manifests as disengaging from, and sustained attention to, this kind of information [56–58]. Meanwhile, it might be worth pointing out that our findings represent some form of hemisphere asymmetries: first, although gray matter volume and

sulcal depth of the bilateral insula were predictive of the level of FNE, only the surface area of its right side was also a predictor [59,60]; second, the volume of the right (but not left) amygdala was another effective predictive feature. These phenomena might be of clinical significance, because some other studies have also observed right-side activation asymmetries among anxious individuals [61–63]. Theoretically, the current findings echo the thoughts of Davidson *et al.* that certain regions of the right hemisphere are specialized for the processing of particular negative emotions and more intense defensive responses [64–67].

Second, a large number of areas in the executive control network were involved in the prediction of BFNE score (specifically, the right middle frontal sulcus, fronto-marginal gyrus and sulcus, inferior and superior frontal gyri, anterior cingulate gyrus and sulcus, and orbital gyrus and sulcus) [68,69]. Recent studies suggest that social anxiety could be better understood from the interaction between the affective network and the executive control network [68]. That is to say, the executive control network is responsible for regulating excessive and inappropriate emotional response to threatening social information [70,71]. As pointed out by Amaral, social anxiety might be raised from dysregulation of the frontal system (which is the center of the executive control network) on normal amygdala function [48]. Jacob *et al.* found that the connectivity between the affective network and the executive control/reappraisal network might be particularly important for SAD diagnosis [72]. It is therefore understandable that multiple regions in this network were highlighted in our results.

Other than that, our RVR analysis also indicated several other brain regions that might be of interest, including the posterior cingulate gyrus/gyri and parahippocampal gyrus. As we mentioned in the Introduction, these regions may not be directly involved in social anxiety, but contribute to the development and maintenance of FNE. The posterior cingulate gyrus sustains memory retrieval (especially for meaningful and emotionally salient events) [73]. More broadly speaking, the posterior cingulate cortex, in which the posterior cingulate gyrus and gyri are located, mediates the interaction between emotion and memory [74,75]. Meanwhile, the parahippocampal gyrus is critical in emotional memory encoding, such as arousal-mediated memory effects [76–78]. Accordingly, we suggest that these regions are associated with the encoding and retrieval of negative social experience, which then reinforce the tendency to avoid being evaluated in social situations (*i.e.,* the behavioral component of FNE).

Noninvasive neuroimaging techniques have contributed to search for quantitative brain-based measurements of psychiatric disorders [79,80]. Nevertheless, neuroimaging markers in psychiatry still lack the level of precision for clinical practice [81]. As pointed out by Etkin, one of the major factors that limited the impact of neuroimaging efforts is the failure in embracing fully data-driven analyses [80]. Here, the findings of this study show that data-driven, machine-learning algorithms and multivariate tools such as the RVR are particularly suitable for examining neural mechanisms underlying complex traits [82–84]. RVR offers a good way to measure interactions between structural features and psychological measures beyond that of traditional univariate brain mapping approaches, and has great potentials to aid in diagnosis across clinical care contexts [84]. We expect that the RVR, as well as other multivariate predictive models, would be critical for the relevant field to move toward a translational neuroscience era [39].

A few limitations of this paper should be addressed. First, while our results reveal a broad range of brain areas that are predictive of individual level of FNE, the functional connectivity between these areas is unknown. Consequently, it is undetermined whether some (or all) of these areas are organized into large-scale neural networks underlying FNE. As we pointed out before, research on within- and between-network connectivities in social anxiety has been fruitful in recent years [85–87]. We therefore encourage future studies to take functional connections between the brain areas highlighted by RVR prediction into account. Second, combining data from different modalities (*e.g.*, not only structural but also functional data) may further improve the performance of our prediction model. Third, our prediction was obtained from a non-clinical sample; therefore, it remains unclear whether the same biomarkers are also effective among patients who are clinically diagnosed with SAD. Finally, there are three versions of the BFNE in previous psychometric studies (*i.e.*, two 8-item variants and a 12-item variant), and it is debated which of these versions is most suitable to adequately measure FNE [88,89]. Carleton *et al.* suggested that the validity of the 12-item variant was actually inferior or comparable to the two 8-item variants [5]. Taking these issues into account, the reliability of the current findings (which were based on the 12-item variant) should be re-examined in follow-up research.

In summary, applying RVR on structural MRI features has resulted in new discovery of biomarkers of FNE. Various regions across the brain were predictive of FNE on the individual level, which might be related to different aspects of its psychological mechanisms. We argue that these findings serve as a starting point that would inspire further investigation to improve prediction

accuracy and generalizability. They may also provide insights into neurobiology of social anxiety and potential targets for pharmacotherapy. The current findings, together with other recent studies [90–93], indicate that researchers are on the verge of a detailed, systematic brain map of anxiety, which covers from primitive subcortical mechanisms to sophisticated cortical processes [94].

MATERIALS AND METHODS

Participants

Two hundred and eighteen adult participants (59 females; age 22.10 ± 2.49 years, range: 18 –36 years) were recruited. All the participants were right handed, and all were clear of organic brain diseases or any abnormal nervous system manifestations. The study was conducted in accordance with the 1964 Declaration of Helsinki and its later amendments, and was approved by the Ethics Committee of Beijing Normal University. Written informed consent was obtained from all participants.

Brief fear of negative evaluation scale

To assess individual differences in fear of negative evaluation, we administered the brief version of the BFNE [95]. The BFNE consists of 12 items, and each item is scored on a five-point Likert scale ranging from 1 ("not at all characteristic of me") to 5 ("extremely characteristic of me"). The reliability and validity of the BFNE have been demonstrated by previous studies [96,97]. People scoring higher on the BFNE scale are more prone to avoid the prospect of being evaluated unfavorably. The Cronbach's alpha coefficient of the scale was 0.89 in the current sample.

Magnetic resonance imaging (MRI) data acquisition

Images were acquired with a Siemens TRIO 3-Tesla scanner at the Beijing Normal University Imaging Center for Brain Research. High-resolution structural images were acquired through a 3D sagittal T1-weighted magnetization-prepared rapid acquisition with gradient-echo (MPRAGE) sequence, using the following parameters: sagittal slices, 144; TR, 2530 ms; TE, 3.39 ms; slice thickness, 1.33 mm; voxel size, $1 \times 1 \times 1.33$ mm^3; flip angle, 7°; inversion time, 1,100 ms; FOV, 256×256 mm^2.

Image processing

Individual T1-weighted MRI images were preprocessed and parceled/segmented with the standard (recon-all) pipeline in Freesurfer version 6.0 [98]. Four measures were calculated for each of the 148 cortical regions across hemispheres according to the Destrieux atlas (Fig. 4) [99], including gray matter volume, cortical thickness, sulcal depth, and surface area. Moreover, volume measures of 17 subcortical regions across hemispheres were also extracted.

Development of prediction model

The morphological measures derived from cortical and subcortical regions (n = 609) were concatenated to yield a feature vector for each participant. The relationship between BFNE scores and brain morphometry was examined using multivariate RVR as implemented in PRoNTo and in-house scripts running under Matlab environment (Mathworks, 2016 release). RVR is a sparse kernel learning multivariate regression method set in a fully probabilistic Bayesian framework [35]. In this framework, a zero-mean Gaussian prior is introduced over the model weights, and is governed by a set of hyper-parameters, one for each weight. The most probable values for these hyper-parameters are then iteratively estimated from the training data, with sparseness achieved due to posterior distributions of many of the weights peaking sharply around zero. Those training vectors associated with non-zero weights are referred to as "relevance" vectors. The optimized posterior distribution of the weights can then be used to predict the target value (*e.g.,* anxiety score) for a previously unseen feature vector, by computing the predictive distribution [35].

In the current work, a leave-one-out cross validation (LOOCV) was used to evaluate the out-of-sample prediction performance. $N-1$ participants (where N is the number of participants) were used as the training set, with the remaining individual used as the testing sample. During the training procedure, each feature was linearly scaled to a range of zero to one across the training set, and then an RVR prediction model was constructed using this training set. During the testing procedure, each testing participant's feature vector was scaled using the scaling parameter acquired during the training procedure. Following this, the RVR prediction model was used to predict the testing participant's BFNE score [100]. The training and testing procedures were repeated for N times such that each participant was used once as the testing participant.

Evaluating the performance of the model

The accuracy of prediction was measured with frequently used statistics [100,101]: (i) the correlation

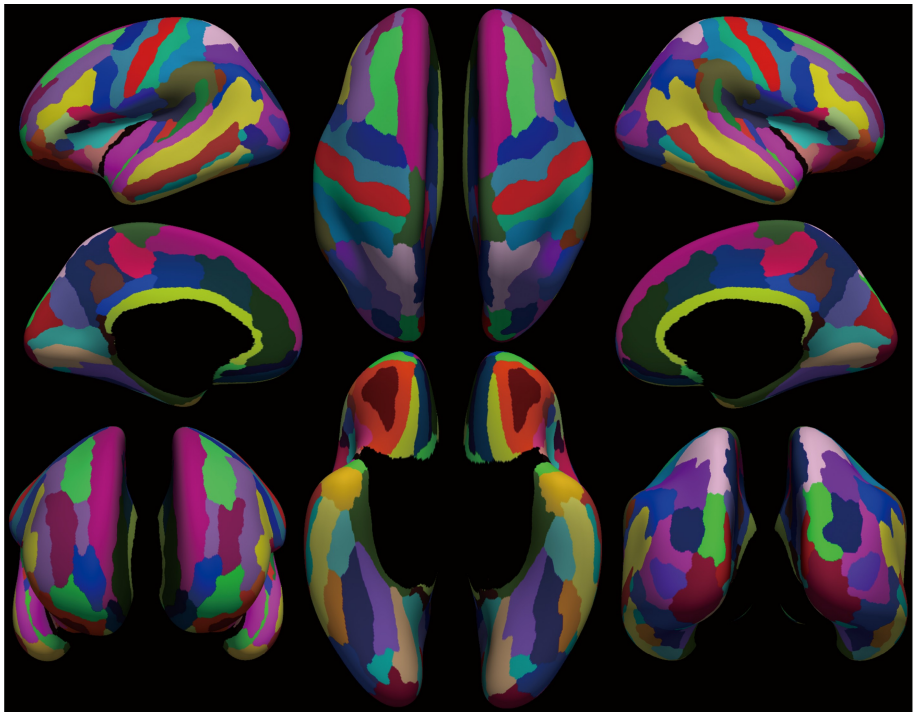

Figure 4. Brain regions in the Destrieux atlas.

coefficient (*r*); and (ii) mean absolute error (*MAE*). The permutation test was applied to determine whether the obtained metrics were significantly better than those expected by chance. More specially, we permuted BFNE scores across training samples without replacement for 1000 times, and each time re-applied the above LOOCV prediction procedure. The permutation resulted in a distribution of *r* and *MAE* values reflecting the null hypothesis that the model did not exceed chance level. The number of times that the permuted value was greater than (or, with respect to *MAE*, less than) the true value, was then divided by 1000, providing an estimated *P*-value for each statistic. Note that a control analysis was implemented to examine the significance of predictions for the model, so as to control for potential confounds of age, gender, and total intracranial volume. In particular, the association between actual and predicted BFNE scores was computed based on the residuals after adjusting for these confounding variables [83,102].

Contributing features and corresponding weights of the model

To quantify the contribution of each feature to prediction, we constructed a new RVR model using all participants. The absolute value of the RVR weight of each feature quantifies its contribution to the model [100,103]. Please note that RVR calculates the weight for samples. As RVR is a sparse model in the sample space, most weight will be zero; the remaining samples with non-zero weight were used to fit the model. The regression coefficients of all features were determined as the weighted sum of the feature vector of the non-zero weighted samples [100,103]. A larger absolute value of weight indicates a greater contribution of the corresponding feature to prediction, in the context of every other feature [100,103,104]. The feature was selected for visualization if the absolute value of its weight was higher than 10% of the maximum absolute weight value. We applied this threshold to eliminate noise components for a better visualization of the most discriminating regions [100,104].

Model validation

A 10-fold cross-validation was applied to re-estimate the prediction performance for validation purpose. All participants were divided into 10 subsets, in which nine were used as the training sets, and the remaining one was used as the testing set. The training set was scaled and used to train an RVR prediction model, which was then used to predict the scores for the scaled testing data. The scaling of testing data used parameters acquired from training data. This procedure was repeated for 10 times, so that each subset was used as testing set once. Finally, the correlation *r* and *MAE* between the true and predicted scores were calculated

across all participants. Since the full dataset was randomly divided into 10 subsets, performance might have depended on data division. Therefore, the 10-fold cross-validation was repeated for 100 times, and the results averaged to produce a final prediction performance. A permutation test was applied 1000 times to test the significance of the prediction performance.

AUTHOR CONTRIBUTIONS

CF conceived the experiment, performed the experiment, collected the data, and analyzed the data. CF, FK, RG, and WL wrote the manuscript.

ACKNOWLEDGEMENTS

This work was supported by the National Natural Science Foundation of China (Nos. 31900757, 32071083 and 32020103008), the Major Program of the Chinese National Social Science Foundation (No. 17ZDA324), and the Youth Innovation Promotion Association, CAS (No. 2019088).

COMPLIANCE WITH ETHICS GUIDELINES

The authors Chunliang Feng, Frank Krueger, Ruolei Gu and Wenbo Luo declare that they have no conflict of interest.

All procedures performed in this study were in accordance with the 1964 Helsinki declaration and its later amendments or comparable ethical standards. The local ethics committee approved the experimental protocol.

REFERENCES

1. American-Psychiatric-Association. (2013) Diagnostic and Statistical Manual of Mental Disorders (DSM-5®). Arlington, VA: American Psychiatric Publishing
2. Clark, D. M. and Wells, A. (1995) A cognitive model of social phobia. In: Social phobia: Diagnosis, Assessment, and Treatment, Heimberg, R. G., Liebowitz, M. R., Hope, D. A. and Schneier, F. R. (Eds.), pp. 69–93, New York: Guilford Press
3. Rapee, R. M. and Heimberg, R. G. (1997) A cognitive-behavioral model of anxiety in social phobia. Behav. Res. Ther., 35, 741−756
4. Watson, D. and Friend, R. (1969) Measurement of social-evaluative anxiety. J. Consult. Clin. Psychol., 33, 448−457
5. Carleton, R. N., Collimore, K. C., McCabe, R. E. and Antony, M. M. (2011) Addressing revisions to the brief fear of negative evaluation scale: measuring fear of negative evaluation across anxiety and mood disorders. J. Anxiety Disord., 25, 822−828
6. Winton, E. C., Clark, D. M. and Edelmann, R. J. (1995) Social anxiety, fear of negative evaluation and the detection of negative emotion in others. Behav. Res. Ther., 33, 193−196
7. Wells, A., Clark, D. M., Salkovskis, P., Ludgate, J., Hackmann, A. and Gelder, M. (1995) Social phobia: The role of in-situation safety behaviors in maintaining anxiety and negative beliefs. Behav. Ther., 26, 153−161
8. Weeks, J. W., Heimberg, R. G., Fresco, D. M., Hart, T. A., Turk, C. L., Schneier, F. R. and Liebowitz, M. R. (2005) Empirical validation and psychometric evaluation of the brief fear of negative evaluation scale in patients with social anxiety disorder. Psychol. Assess., 17, 179−190
9. Miskovic, V. and Schmidt, L. A. (2012) Social fearfulness in the human brain. Neurosci. Biobehav. Rev., 36, 459−478
10. LeDoux, J. E. (2000) Emotion circuits in the brain. Annu. Rev. Neurosci., 23, 155−184
11. LeDoux, J. (2003) The emotional brain, fear, and the amygdala. Cell. Mol. Neurobiol., 23, 727−738
12. Marek, R., Strobel, C., Bredy, T. W. and Sah, P. (2013) The amygdala and medial prefrontal cortex: partners in the fear circuit. J. Physiol., 591, 2381−2391
13. Bishop, S., Duncan, J., Brett, M. and Lawrence, A. D. (2004) Prefrontal cortical function and anxiety: controlling attention to threat-related stimuli. Nat. Neurosci., 7, 184−188
14. Bishop, S. J. (2007) Neurocognitive mechanisms of anxiety: an integrative account. Trends Cogn. Sci., 11, 307−316
15. Bishop, S. J. (2009) Trait anxiety and impoverished prefrontal control of attention. Nat. Neurosci., 12, 92−98
16. Kim, M. J., Gee, D. G., Loucks, R. A., Davis, F. C. and Whalen, P. J. (2011) Anxiety dissociates dorsal and ventral medial prefrontal cortex functional connectivity with the amygdala at rest. Cereb. Cortex, 21, 1667−1673
17. Kim, M. J. and Whalen, P. J. (2009) The structural integrity of an amygdala-prefrontal pathway predicts trait anxiety. J. Neurosci., 29, 11614−11618
18. Paulus, M. P. and Stein, M. B. (2006) An insular view of anxiety. Biol. Psychiatry, 60, 383−387
19. Stein, M. B., Simmons, A. N., Feinstein, J. S. and Paulus, M. P. (2007) Increased amygdala and insula activation during emotion processing in anxiety-prone subjects. Am. J. Psychiatry, 164, 318−327
20. Baur, V., Hänggi, J., Langer, N. and Jäncke, L. (2013) Resting-state functional and structural connectivity within an insula-amygdala route specifically index state and trait anxiety. Biol. Psychiatry, 73, 85−92
21. Straube, T., Kolassa, I. T., Glauer, M., Mentzel, H. J. and Miltner, W. H. (2004) Effect of task conditions on brain responses to threatening faces in social phobics: an event-related functional magnetic resonance imaging study. Biol. Psychiatry, 56, 921−930
22. Lira Yoon, K., Fitzgerald, D. A., Angstadt, M., McCarron, R. A. and Phan, K. L. (2007) Amygdala reactivity to emotional faces at high and low intensity in generalized social phobia: a 4-Tesla functional MRI study. Psychiatry Res., 154, 93−98
23. Stein, M. B., Goldin, P. R., Sareen, J., Zorrilla, L. T. and Brown, G. G. (2002) Increased amygdala activation to angry and contemptuous faces in generalized social phobia. Arch. Gen. Psychiatry, 59, 1027−1034
24. Blair, K. S., Geraci, M., Otero, M., Majestic, C., Odenheimer, S., Jacobs, M., Blair, R. J. and Pine, D. S. (2011) Atypical modulation of medial prefrontal cortex to self-referential comments in generalized social phobia. Psychiatry Res., 193,

38−45
25. Boehme, S., Ritter, V., Tefikow, S., Stangier, U., Strauss, B., Miltner, W. H. and Straube, T. (2014) Brain activation during anticipatory anxiety in social anxiety disorder. Soc. Cogn. Affect. Neurosci., 9, 1413−1418
26. Izuma, K., Saito, D. N. and Sadato, N. (2008) Processing of social and monetary rewards in the human striatum. Neuron, 58, 284−294
27. Izuma, K., Saito, D. N. and Sadato, N. (2010) Processing of the incentive for social approval in the ventral striatum during charitable donation. J. Cogn. Neurosci., 22, 621−631
28. Nutt, D. J., Bell, C. J. and Malizia, A. L. (1998) Brain mechanisms of social anxiety disorder. J. Clin. Psychiatry, 59, 4−11
29. Blackford, J. U. and Pine, D. S. (2012) Neural substrates of childhood anxiety disorders: a review of neuroimaging findings. Child Adolesc. Psychiatr. Clin. N. Am., 21, 501−525
30. Mochcovitch, M. D., da Rocha Freire, R. C., Garcia, R. F. and Nardi, A. E. (2014) A systematic review of fMRI studies in generalized anxiety disorder: evaluating its neural and cognitive basis. J. Affect. Disord., 167, 336−342
31. Domschke, K. and Dannlowski, U. (2010) Imaging genetics of anxiety disorders. Neuroimage, 53, 822−831
32. Grupe, D. W. and Nitschke, J. B. (2013) Uncertainty and anticipation in anxiety: an integrated neurobiological and psychological perspective. Nat. Rev. Neurosci., 14, 488−501
33. Xia, F. and Kheirbek, M. A. (2020) Circuit-based biomarkers for mood and anxiety disorders. Trends Neurosci., 43, 902−915
34. Dafflon, J., Pinaya, W. H. L., Turkheimer, F., Cole, J. H., Leech, R., Harris, M. A., Cox, S. R., Whalley, H. C., McIntosh, A. M. and Hellyer, P. J. (2020) An automated machine learning approach to predict brain age from cortical anatomical measures. Hum. Brain Mapp., 41, 3555−3566
35. Tipping, M. E. (2001) Sparse Bayesian learning and the relevance vector machine. J. Mach. Learn. Res., 1, 211−244
36. Li, S., Yuan, X., Pu, F., Li, D., Fan, Y., Wu, L., Chao, W., Chen, N., He, Y. and Han, Y. (2014) Abnormal changes of multidimensional surface features using multivariate pattern classification in amnestic mild cognitive impairment patients. J. Neurosci., 34, 10541−10553
37. Ecker, C., Marquand, A., Mourão-Miranda, J., Johnston, P., Daly, E. M., Brammer, M. J., Maltezos, S., Murphy, C. M., Robertson, D., Williams, S. C., *et al*. (2010) Describing the brain in autism in five dimensions-magnetic resonance imaging-assisted diagnosis of autism spectrum disorder using a multiparameter classification approach. J. Neurosci., 30, 10612−10623
38. Westman, E., Aguilar, C., Muehlboeck, J. S. and Simmons, A. (2013) Regional magnetic resonance imaging measures for multivariate analysis in Alzheimer's disease and mild cognitive impairment. Brain Topogr., 26, 9−23
39. Sui, J., Jiang, R., Bustillo, J. and Calhoun, V. (2020) Neuroimaging-based individualized prediction of cognition and behavior for mental disorders and health: Methods and promises. Biol. Psychiatry, 88, 818−828
40. Cheng, B., Zhang, D., Chen, S., Kaufer, D. I., Shen, D., and the Alzheimer's Disease Neuroimaging Initiative. (2013) Semi-supervised multimodal relevance vector regression improves cognitive performance estimation from imaging and biological biomarkers. Neuroinformatics, 11, 339−353
41. Feng, C., Cui, Z., Cheng, D., Xu, R. and Gu, R. (2019) Individualized prediction of dispositional worry using white matter connectivity. Psychol. Med., 49, 1999−2008
42. Xu, J., Van Dam, N. T., Feng, C., Luo, Y., Ai, H., Gu, R. and Xu, P. (2019) Anxious brain networks: A coordinate-based activation likelihood estimation meta-analysis of resting-state functional connectivity studies in anxiety. Neurosci. Biobehav. Rev., 96, 21−30
43. Yeo, B. T., Krienen, F. M., Sepulcre, J., Sabuncu, M. R., Lashkari, D., Hollinshead, M., Roffman, J. L., Smoller, J. W., Zöllei, L., Polimeni, J. R., *et al*. (2011) The organization of the human cerebral cortex estimated by intrinsic functional connectivity. J. Neurophysiol., 106, 1125−1165
44. Sheline, Y. I., Price, J. L., Yan, Z. and Mintun, M. A. (2010) Resting-state functional MRI in depression unmasks increased connectivity between networks via the dorsal nexus. Proc. Natl. Acad. Sci. USA, 107, 11020−11025
45. Choi, E. Y., Yeo, B. T. and Buckner, R. L. (2012) The organization of the human striatum estimated by intrinsic functional connectivity. J. Neurophysiol., 108, 2242−2263
46. Buckner, R. L., Krienen, F. M., Castellanos, A., Diaz, J. C. and Yeo, B. T. (2011) The organization of the human cerebellum estimated by intrinsic functional connectivity. J. Neurophysiol., 106, 2322−2345
47. Sang, L., Qin, W., Liu, Y., Han, W., Zhang, Y., Jiang, T. and Yu, C. (2012) Resting-state functional connectivity of the vermal and hemispheric subregions of the cerebellum with both the cerebral cortical networks and subcortical structures. Neuroimage, 61, 1213−1225
48. Amaral, D. G. (2002) The primate amygdala and the neurobiology of social behavior: implications for understanding social anxiety. Biol. Psychiatry, 51, 11−17
49. Hahn, A., Stein, P., Windischberger, C., Weissenbacher, A., Spindelegger, C., Moser, E., Kasper, S. and Lanzenberger, R. (2011) Reduced resting-state functional connectivity between amygdala and orbitofrontal cortex in social anxiety disorder. Neuroimage, 56, 881−889
50. Duval, E. R., Joshi, S. A., Russman Block, S., Abelson, J. L. and Liberzon, I. (2018) Insula activation is modulated by attention shifting in social anxiety disorder. J. Anxiety Disord., 56, 56−62
51. Klumpp, H., Post, D., Angstadt, M., Fitzgerald, D. A. and Phan, K. L. (2013) Anterior cingulate cortex and insula response during indirect and direct processing of emotional faces in generalized social anxiety disorder. Biol. Mood Anxiety Disord., 3, 7
52. Phan, K. L., Fitzgerald, D. A., Nathan, P. J. and Tancer, M. E. (2006) Association between amygdala hyperactivity to harsh

faces and severity of social anxiety in generalized social phobia. Biol. Psychiatry, 59, 424−429
53. Bas-Hoogendam, J. M., van Steenbergen, H., van der Wee, N. J. A. and Westenberg, P. M. (2020) Amygdala hyperreactivity to faces conditioned with a social-evaluative meaning− a multiplex, multigenerational fMRI study on social anxiety endophenotypes. Neuroimage Clin., 26, 102247
54. Klumpp, H., Angstadt, M. and Phan, K. L. (2012) Insula reactivity and connectivity to anterior cingulate cortex when processing threat in generalized social anxiety disorder. Biol. Psychol., 89, 273−276
55. Shah, S. G., Klumpp, H., Angstadt, M., Nathan, P. J. and Phan, K. L. (2009) Amygdala and insula response to emotional images in patients with generalized social anxiety disorder. J. Psychiatry Neurosci., 34, 296−302
56. Rossignol, M., Campanella, S., Bissot, C. and Philippot, P. (2013) Fear of negative evaluation and attentional bias for facial expressions: an event-related study. Brain Cogn., 82, 344−352
57. Birk, S. L., Horenstein, A., Weeks, J., Olino, T., Heimberg, R., Goldin, P. R. and Gross, J. J. (2019) Neural responses to social evaluation: The role of fear of positive and negative evaluation. J. Anxiety Disord., 67, 102114
58. Gu, R., Ao, X., Mo, L. and Zhang, D. (2020) Neural correlates of negative expectancy and impaired social feedback processing in social anxiety. Soc. Cogn. Affect. Neurosci., 15, 285−291
59. Syal, S., Hattingh, C. J., Fouché, J. P., Spottiswoode, B., Carey, P. D., Lochner, C. and Stein, D. J. (2012) Grey matter abnormalities in social anxiety disorder: a pilot study. Metab. Brain Dis., 27, 299−309
60. Kawaguchi, A., Nemoto, K., Nakaaki, S., Kawaguchi, T., Kan, H., Arai, N., Shiraishi, N., Hashimoto, N. and Akechi, T. (2016) Insular volume reduction in patients with social anxiety disorder. Front. Psychiatry, 7, 3
61. Papousek, I. and Schulter, G. (2001) Associations between EEG asymmetries and electrodermal lability in low vs. high depressive and anxious normal individuals. Int. J. Psychophysiol., 41, 105−117
62. Blackhart, G. C., Minnix, J. A. and Kline, J. P. (2006) Can EEG asymmetry patterns predict future development of anxiety and depression? A preliminary study. Biol. Psychol., 72, 46−50
63. Aftanas, L. I. and Pavlov, S. V. (2005) Trait anxiety impact on posterior activation asymmetries at rest and during evoked negative emotions: EEG investigation. Int. J. Psychophysiol., 55, 85−94
64. Davidson, R. J. and Fox, N. A. (1982) Asymmetrical brain activity discriminates between positive and negative affective stimuli in human infants. Science, 218, 1235−1237
65. Davidson, R. J. and Fox, N. A. (1989) Frontal brain asymmetry predicts infants' response to maternal separation. J. Abnorm. Psychol., 98, 127−131
66. Kalin, N. H., Larson, C., Shelton, S. E. and Davidson, R. J. (1998) Asymmetric frontal brain activity, cortisol, and behavior associated with fearful temperament in rhesus monkeys. Behav. Neurosci., 112, 286−292
67. Wheeler, R. E., Davidson, R. J. and Tomarken, A. J. (1993) Frontal brain asymmetry and emotional reactivity: a biological substrate of affective style. Psychophysiology, 30, 82−89
68. Geiger, M. J., Domschke, K., Ipser, J., Hattingh, C., Baldwin, D. S., Lochner, C. and Stein, D. J. (2016) Altered executive control network resting-state connectivity in social anxiety disorder. World J. Biol. Psychiatry, 17, 47−57
69. Seeley, W. W., Menon, V., Schatzberg, A. F., Keller, J., Glover, G. H., Kenna, H., Reiss, A. L. and Greicius, M. D. (2007) Dissociable intrinsic connectivity networks for salience processing and executive control. J. Neurosci., 27, 2349−2356
70. Morillas-Romero, A., Tortella-Feliu, M., Balle, M. and Bornas, X. (2015) Spontaneous emotion regulation and attentional control. Emotion, 15, 162−175
71. Tully, L. M., Lincoln, S. H. and Hooker, C. I. (2012) Impaired executive control of emotional information in social anhedonia. Psychiatry Res., 197, 29−35
72. Jacob, Y., Shany, O., Goldin, P. R., Gross, J. J. and Hendler, T. (2019) Reappraisal of interpersonal criticism in social anxiety disorder: A brain network hierarchy perspective. Cereb. Cortex, 29, 3154−3167
73. Binder, J. R. and Desai, R. H. (2011) The neurobiology of semantic memory. Trends Cogn. Sci., 15, 527−536
74. Zhang, D., Lin, Y., Jing, Y., Feng, C. and Gu, R. (2019) The dynamics of belief updating in human cooperation: Findings from inter-brain ERP hyperscanning. Neuroimage, 198, 1−12
75. Nielsen, F. A., Balslev, D. and Hansen, L. K. (2005) Mining the posterior cingulate: segregation between memory and pain components. Neuroimage, 27, 520−532
76. Murty, V. P., Ritchey, M., Adcock, R. A. and LaBar, K. S. (2010) fMRI studies of successful emotional memory encoding: A quantitative meta-analysis. Neuropsychologia, 48, 3459−3469
77. Medford, N., Phillips, M. L., Brierley, B., Brammer, M., Bullmore, E. T. and David, A. S. (2005) Emotional memory: separating content and context. Psychiatry Res., 138, 247−258
78. Erk, S., Kiefer, M., Grothe, J., Wunderlich, A. P., Spitzer, M. and Walter, H. (2003) Emotional context modulates subsequent memory effect. Neuroimage, 18, 439−447
79. Mitelman, S. A. (2019) Transdiagnostic neuroimaging in psychiatry: A review. Psychiatry Res., 277, 23−38
80. Etkin, A. (2019) A reckoning and research agenda for neuroimaging in psychiatry. Am. J. Psychiatry, 176, 507−511
81. Linden, D. E. (2012) The challenges and promise of neuroimaging in psychiatry. Neuron, 73, 8−22
82. Tang, H., Lu, X., Cui, Z., Feng, C., Lin, Q., Cui, X., Su, S. and Liu, C. (2018) Resting-state functional connectivity and deception: Exploring individualized deceptive propensity by machine learning. Neuroscience, 395, 101−112
83. Lu, X., Li, T., Xia, Z., Zhu, R., Wang, L., Luo, Y. J., Feng, C. and Krueger, F. (2019) Connectome-based model predicts individual differences in propensity to trust. Hum. Brain Mapp., 40, 1942−1954
84. Stonnington, C. M., Chu, C., Klöppel, S., Jack, C. R. Jr, Ashburner, J. and Frackowiak, R. S., and the Alzheimer Disease

Neuroimaging Initiative. (2010) Predicting clinical scores from magnetic resonance scans in Alzheimer's disease. Neuroimage, 51, 1405−1413

85. Liu, F., Guo, W., Fouche, J. P., Wang, Y., Wang, W., Ding, J., Zeng, L., Qiu, C., Gong, Q., Zhang, W., *et al*. (2015) Multivariate classification of social anxiety disorder using whole brain functional connectivity. Brain Struct. Funct., 220, 101−115
86. Whitfield-Gabrieli, S., Ghosh, S. S., Nieto-Castanon, A., Saygin, Z., Doehrmann, O., Chai, X. J., Reynolds, G. O., Hofmann, S. G., Pollack, M. H. and Gabrieli, J. D. (2016) Brain connectomics predict response to treatment in social anxiety disorder. Mol. Psychiatry, 21, 680−685
87. Liu, F., Zhu, C., Wang, Y., Guo, W., Li, M., Wang, W., Long, Z., Meng, Y., Cui, Q., Zeng, L., *et al*. (2015) Disrupted cortical hubs in functional brain networks in social anxiety disorder. Clin. Neurophysiol., 126, 1711−1716
88. Fox, R. S., Kwakkenbos, L., Carrier, M. E., Mills, S. D., Gholizadeh, S., Jewett, L. R., Roesch, S. C., Merz, E. L., Assassi, S., Furst, D. E., *et al*. (2018) Reliability and validity of three versions of the brief fear of negative evaluation scale in patients with systemic sclerosis: A scleroderma patient-centered intervention network cohort study. Arthritis Care Res. (Hoboken), 70, 1646−1652
89. Wong, Q. J. and Moulds, M. L. (2014) An examination of the measurement equivalence of the brief fear of negative evaluation scale across individuals who identify with an asian ethnicity and individuals who identify with a European ethnicity. Assessment, 21, 713−722
90. Bach, D. R., Hoffmann, M., Finke, C., Hurlemann, R. and Ploner, C. J. (2019) Disentangling hippocampal and amygdala contribution to human anxiety-like behavior. J. Neurosci., 39, 8517−8526
91. Berry, A. S., White, R. L. 3rd, Furman, D. J., Naskolnakorn, J. R., Shah, V. D., D'Esposito, M. and Jagust, W. J. (2019) Dopaminergic mechanisms underlying normal variation in trait anxiety. J. Neurosci., 39, 2735−2744
92. Fung, B. J., Qi, S., Hassabis, D., Daw, N. and Mobbs, D. (2019) Slow escape decisions are swayed by trait anxiety. Nat. Hum. Behav., 3, 702−708
93. Geng, H., Wang, Y., Gu, R., Luo, Y. J., Xu, P., Huang, Y. and Li, X. (2018) Altered brain activation and connectivity during anticipation of uncertain threat in trait anxiety. Hum. Brain Mapp., 39, 3898−3914
94. McNaughton, N. (2019) Brain maps of fear and anxiety. Nat. Hum. Behav., 3, 662−663
95. Leary, M. R. (1983) A brief version of the fear of negative evaluation scale. Pers. Soc. Psychol. Bull., 9, 371−375
96. Collins, K. A., Westra, H. A., Dozois, D. J. and Stewart, S. H. (2005) The validity of the brief version of the fear of negative evaluation scale. J. Anxiety Disord., 19, 345−359
97. Rodebaugh, T. L., Woods, C. M., Thissen, D. M., Heimberg, R. G., Chambless, D. L. and Rapee, R. M. (2004) More information from fewer questions: the factor structure and item properties of the original and brief fear of negative evaluation scale. Psychol. Assess., 16, 169−181
98. Dale, A. M., Fischl, B. and Sereno, M. I. (1999) Cortical surface-based analysis. I. Segmentation and surface reconstruction. Neuroimage, 9, 179−194
99. Destrieux, C., Fischl, B., Dale, A. and Halgren, E. (2010) Automatic parcellation of human cortical gyri and sulci using standard anatomical nomenclature. Neuroimage, 53, 1−15
100. Gong, Q., Li, L., Du, M., Pettersson-Yeo, W., Crossley, N., Yang, X., Li, J., Huang, X. and Mechelli, A. (2014) Quantitative prediction of individual psychopathology in trauma survivors using resting-state FMRI. Neuropsychopharmacology, 39, 681−687
101. Franke, K., Ziegler, G., Klöppel, S., Gaser, C., and the Alzheimer's Disease Neuroimaging Initiative. (2010) Estimating the age of healthy subjects from T1-weighted MRI scans using kernel methods: exploring the influence of various parameters. Neuroimage, 50, 883−892
102. Feng, C., Zhu, Z., Cui, Z., Ushakov, V., Dreher, J.C., Luo, W., Gu, R., Wu, X. and Krueger, F. (2021) Prediction of trust propensity from intrinsic brain morphology and functional connectome. Hum Brain Mapp. 42, , 175−191
103. Cui, Z. and Gong, G. (2018) The effect of machine learning regression algorithms and sample size on individualized behavioral prediction with functional connectivity features. Neuroimage, 178, 622−637
104. Erus, G., Battapady, H., Satterthwaite, T. D., Hakonarson, H., Gur, R. E., Davatzikos, C. and Gur, R. C. (2015) Imaging patterns of brain development and their relationship to cognition. Cereb. Cortex, 25, 1676−1684